Future Batteries 6 (2025) 100058

Contents lists available at ScienceDirect

Future Batteries

journal homepage: www.sciencedirect.com/journal/future-batteries

Mechanistic insight into defective molybdenum carbide as cathode catalyst in Li-CO_2 battery

Tingting Zhao [a], Lixiang Yan [a], Xueying Qiu [a], Liubin Song [a,*], Yanmei Nie [a], Yiyu Xiong [a], Ao Li [a], Yukang Su [a], Likai Yan [b,*]

[a] School of Chemistry and Chemical Engineering, Changsha University of Science and Technology, Changsha 410114, PR China
[b] Institute of Functional Materials Chemistry and Local United Engineering Lab for Power Battery, Faculty of Chemistry, Northeast Normal University, Changchun 130024, PR China

ARTICLE INFO

Keywords:
Li-CO_2 batteries
Cathode catalyst
Defective molybdenum carbide material
Density functional theory
Reaction mechanism

ABSTRACT

Li-CO_2 batteries have significant advantages, including high theoretical capacity and environmental friendliness, making them promising next-generation energy storage device with substantial capacity. However, the lack of efficient cathode catalysts hampers the rate of CO_2 reduction/evolution reactions (CRR/CER), significantly impeding its progress. Herein, by means of density functional theory (DFT) calculations, the potential mechanism of defective molybdenum carbide (V_C-Mo_2C) as cathode catalysts in Li-CO_2 batteries was systematically investigated. The results reveal that V_C-Mo_2C effectively suppresses the formation of Li_2CO_3, thereby promoting the preferential generation of $Li_2C_2O_4$ products in the overall reaction. This study aims to offer insight into the development of cathode catalysts for Li-CO_2 batteries.

1. Introduction

The extensive utilization of conventional fossil fuels has resulted in significant CO_2 emissions, which not only exacerbates the greenhouse effect but also accelerates the depletion of energy resources. Li-CO_2 batteries exhibit promising potential for alleviating the energy crisis and reducing environmental pollution due to their distinctive energy storage capacity and carbon sequestration function. Employing lithium metal as the anode, Li-CO_2 batteries facilitate the migration of lithium ions (Li^+) from the negative electrode during discharge, enabling them to react with CO_2 and generate stable solid products, thereby accomplishing both efficient energy storage and effective CO_2 capture [1]. Boasting advantages such as high theoretical energy density (1876 Wh/kg) and proficient CO_2 capture capability, Li-CO_2 batteries emerge as prospective candidates for applications in new energy vehicles, aerospace exploration, deep-sea exploration [2–4]. Nevertheless, commercial development of Li-CO_2 batteries is severely constrained by sluggish reaction kinetics leading to elevated overpotential and diminished energy efficiency [5,6].

In order to reduce overpotential and enhance the reaction kinetics of Li-CO_2 batteries, researchers are actively exploring innovative strategies. Among these strategies, incorporating catalysts on the cathode to facilitate CO_2 reduction/evolution reactions (CRR/CER) appears most promising in terms of enhancing battery performance [7–9]. Commonly employed catalysts for the cathode include carbon nanomaterials [3,10,11], platinum group metal catalysts [12,13], oxides [14–17], covalent organic frameworks [18], metal sulfides [19–21]. Ankit K. Chourasia et al. [10] developed a heteroatom-doped hierarchical porous candle soot carbon with exceptional electrochemical performance, a total discharge capacity of 11490 mAh g^{-1} at a high initial discharge voltage of 2.75 V and a current density of 200 mA g^{-1} However, a major challenge arises from the formation of Li_2CO_3 as the final discharge product on the surface of these cathode catalysts. Li_2CO_3 exhibits slow decomposition kinetics during charging (especially at high charging voltages up to 4.3 V relative to Li/Li^+), leading to difficulties in CO_2 release on the cathode side of Li-CO_2 batteries [22].

The latest research has revealed that the intermediate product $Li_2C_2O_4$, found on the surface of cathode catalysts, exhibits lower overpotential and improved decomposability [23,24]. $Li_2C_2O_4$ as the final discharge product can significantly enhance the reaction rate of Li-CO_2 batteries. However, only a few catalysts have better selectivity for producing $Li_2C_2O_4$, such as molybdenum-based catalysts [25]. Hou et al. [23] used Mo_2C/CNT as the cathode catalyst for Li-CO_2 systems and demonstrated its ability to stabilize the intermediate reduction

* Corresponding authors.
E-mail addresses: liubinsong1981@126.com (L. Song), yanlk924@nenu.edu.cn (L. Yan).

https://doi.org/10.1016/j.fub.2025.100058
Received 4 November 2024; Received in revised form 4 March 2025; Accepted 12 March 2025
Available online 15 March 2025

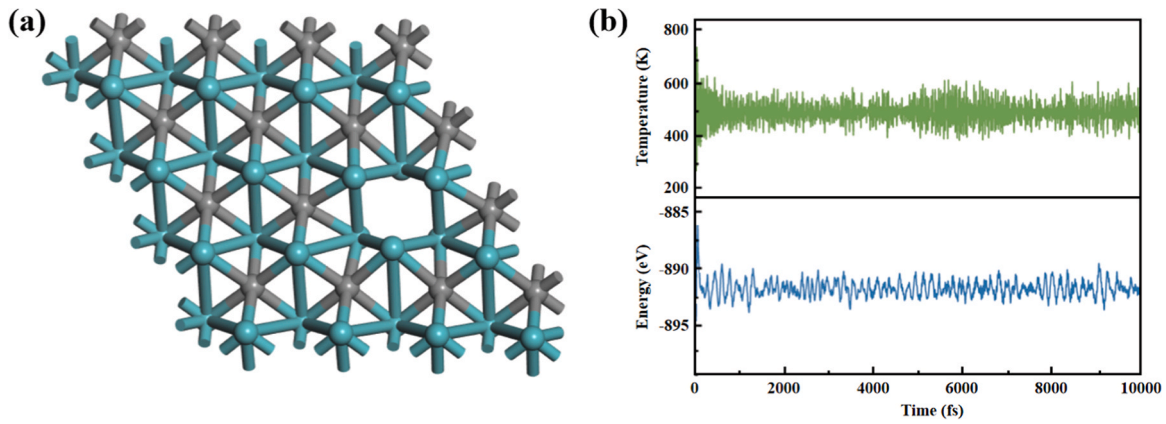

Fig. 1. (a) The optimized V_C-Mo_2C structure model; (b) variations of temperature and energy against time for AIMD simulations of V_C-Mo_2C.

product $Li_2C_2O_4$ during discharge. Zhou et al. [24] show that the intermediate discharge product $Li_2C_2O_4$ stabilized by Mo_2C via coordinative electrons transfer should be responsible for the reduction of overpotential. Yang et al. [26] found that when Mo_2C is used as a cathode catalyst, $Li_2C_2O_4$ can act as the final discharge product and prevents the formation of Li_2CO_3. To enhance catalytic activity, researchers have implemented strategies such as defect introduction [27, 28], metal doping [29], and surface modification [30], yielding certain effects. Carbon defects are structural factors influencing the catalytic activity of transition-metal carbides, which can not only facilitate the conversion of CO_2 but also accelerate the transport of Li^+ [31]. Therefore, the introduction of defects is of great significance for improving the activity of the cathode catalyst in Li-CO_2 batteries. This paper explores the influence mechanism and performance of V_C-Mo_2C as a cathode catalyst for Li-CO_2 batteries, aiming to offer new novel insights and theoretical support for research on V_C-Mo_2C cathode catalysts.

2. Computational methods and models

All the calculations were performed using the DFT framework, which are implemented in the $Dmol^3$ code [32,33]. The generalized gradient approximation (GGA) using the Perdew–Burke–Ernzerhof (PBE) parameterization was used to describe electronic exchange and correlation effects [34]. The DFT semi-core pseudopotential (DSPP) method was employed to treat the relativistic effect of transition metals by introducing some degree of relativistic corrections to replace the core electrons using a single effective potential [35]. To accurately describe the weak interactions of CRR species with catalysts, the PBE+D2 method with the Grimme vdW correction was employed [36]. Self-consistent field (SCF) computations were performed with a convergence criterion of 10^{-6} a.u. on the total energy and electronic computations. The Brillouin zone integration was performed with $5 \times 5 \times 1$ *k*-points for geometry optimizations. A conductor-like screening model (COSMO) was used to simulate the H_2O solvent environment throughout the whole process, whose dielectric constant was set as 78.54 [37]. The vacuum space in the z direction was set as 20 Å, which is sufficiently large to avoid the interlayer interaction. The free energy change (G) of each elementary reaction step during CRR was calculated according to the computational hydrogen electrode (CHE) model suggested by Nørskov and co-worker [38,39]. In this method, the free energy change is defined as: $\Delta G = \Delta E + \Delta E_{ZPE} - T\Delta S$, where ΔE is the electronic energy difference directly determined by DFT calculations, ΔE_{ZPE} is the change in the zero-point energy, T is the temperature (298.15 K), and ΔS is the change in entropy. The zero-point energies and the total entropies of the CRR intermediates were computed from the vibrational frequencies. The entropies and vibrational frequencies of the molecules (including CO_2, etc.) in the gas phase were taken from the NIST database, while the vibrational frequencies of the adsorbed species to obtain ZPE contribution in the free energy expression were computed. The vibrational modes of the adsorbate were computed explicitly, while the catalyst sheet was fixed (assuming that the vibrations of the substrate are negligible).

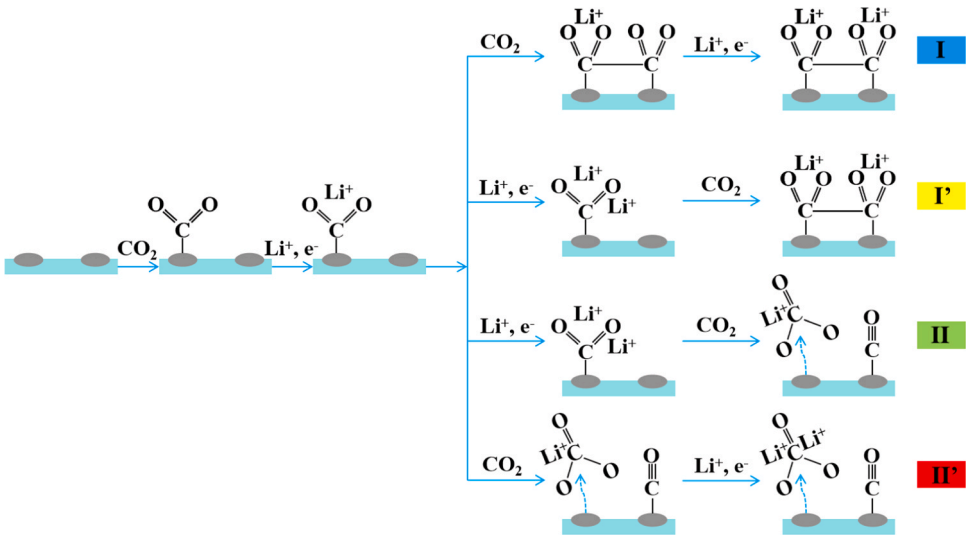

Fig. 2. All possible reaction paths on the surface of V_C-Mo_2C catalyst.

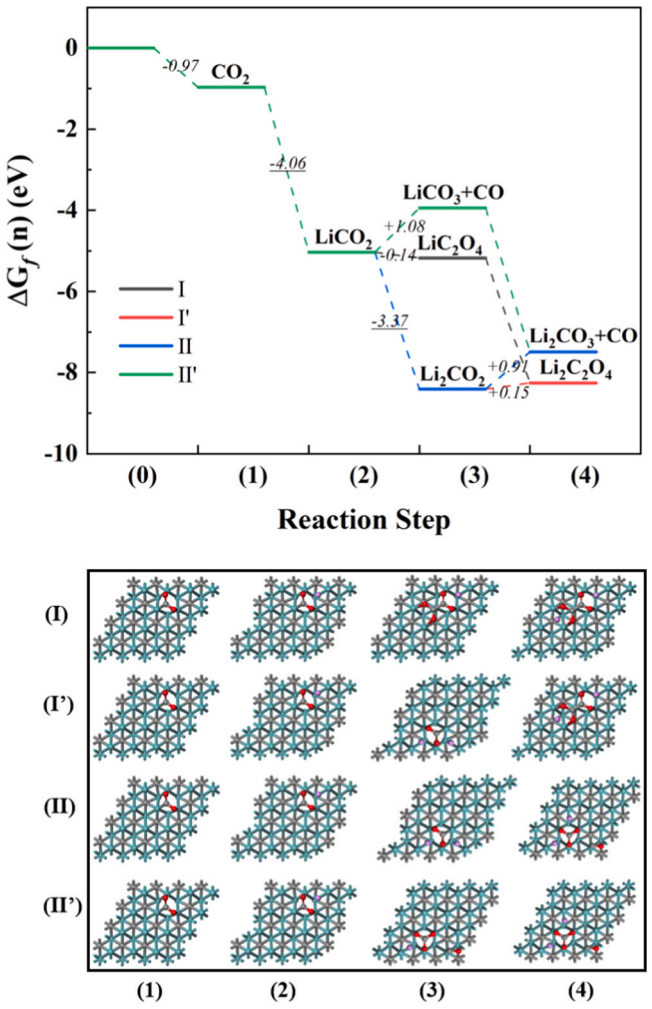

Fig. 3. Gibbs free energy spectra and intermediate product models of all reaction paths on V_C-Mo_2C.

3. Results and discussion

3.1. Geometric structures and stabilities

To investigate the effect of defect location on the catalytic performance of V_C-Mo_2C, we calculated the formation energies of C and Mo defects according to the formula: $E_f(V_C) = E_{V_C-Mo_2C} - E_{Mo_2C} + n\mu_C$. According to calculations, the formation energies of C and Mo defects are 8.77 eV and 9.50 eV, respectively. The calculation results indicate that C defects are more likely to form, making them more commonly used in catalysts, which is consistent with previous research findings [40]. The crystal structure of V_C-Mo_2C can be considered as a sandwich-like structure, where the atoms of adjacent vacancies are slightly displaced inward due to the introduction of C vacancies. The optimized structure of V_C-Mo_2C is illustrated in Fig. 1a. The optimized lattice parameters for V_C-Mo_2C are a=b= 12.1884/4 = 3.0471 Å, which is consistent with experimental values (a=b=3.006 Å), indicating the reliability of our methodology [32].

The thermodynamic stability of V_C-Mo_2C was further evaluated using Ab initio molecular dynamics (AIMD) simulation [41] at 500 K with a time step 1.0 fs for a total 10 ps. The energy and temperature oscillate within small ranges and no significant structural deformation is observed after 10000 steps, indicating V_C-Mo_2C has high thermodynamic stability, as shown in Fig. 1b.

3.2. Gibbs free energy changes

The Gibbs free energy of nucleation for all potential reaction pathways on V_C-Mo_2C surface (Fig. 2) was computed at open circuit potential (U=0 V), as depicted in Fig. 3. Among these pathways, steps involving Li^+ and concurrent electron transfer exhibit a downhill trend in the Gibbs free energy. Pathways I and I′ lead $Li_2C_2O_4$ as the ultimate product, whereas pathways II and II' produce Li_2CO_3 as the final product. The adsorption and activation of CO_2 on the V_C-Mo_2C catalyst substrate represent the initial step in the Li-CO_2 battery conversion reaction [42]. In the subsequent reaction, Li^+ interacts with surface-bound CO_2 on V_C-Mo_2C to form an intermediate species denoted as *$LiCO_2$. The third reaction step encompasses three potential pathways: *$LiCO_2$ undergoes electron transfer and reacts with Li^+ to yield *Li_2CO_2; alternatively, it can react with CO_2 to generate *LiC_2O_4; or, through a reaction between *$LiCO_3$ and CO, give rise to both *$LiCO_3$ and *CO. Gibbs free energy changes for pathway I, pathway I′, and pathway II in this third step are −0.14 eV, −3.37 eV, −3.37 eV respectively, indicating their favorable occurrence. However, the Gibbs free energy curve for pathway II' exhibits an upward trend due to a higher formation barrier associated with the C≡O bond during pathway II'. Pathway I′ and pathway II exhibit significantly larger Gibbs free energy changes compared to pathway I due to their involvement of electron transfer processes; consequently, intermediate reactions predominantly occur along pathways I′ and II. The nucleation steps of $Li_2C_2O_4$ and Li_2CO_3 are represented by the fourth step. Yang et al. [26] conducted calculations on the Gibbs free energy changes for each reaction step involved in the formation of $Li_2C_2O_4$ and Li_2CO_3 on V_C-Mo_2C. Their results demonstrate that the Gibbs free energy required for CO_2 to react with Li_2CO_2, forming $Li_2C_2O_4$, is smaller compared to that needed for generating Li_2CO_3. Specifically, pathway I′ in the fourth reaction step exhibits a change in free energy of + 0.18 eV, while pathway II generates a change in free energy of + 0.91 eV resulting in the production of Li_2CO_3. The higher free energy requirement for generating Li_2CO_3 suggests that it is less likely to form compared to $Li_2C_2O_4$. In order to estimate the selectivity of different pathways, the Boltzmann distribution formula $\exp[(\Delta G)/(k_BT)]$ was adopted on the basis of their free energy difference, where ΔG= 0.91/0.18 eV and T = 298.15 K. The $Li_2C_2O_4$: Li_2CO_3 molar ratio is ~ (2.133×10^{12}): 1 at ambient temperature, indicating a high selectivity toward the $Li_2C_2O_4$, so Li_2CO_3 step is not considered.

Under the equilibrium potentials of $Li_2C_2O_4$ (U =U_0 ($Li_2C_2O_4$) = 3.01 V) and Li_2CO_3 (U = U_0 (Li_2CO_3) = 2.87 V) nucleations, all steps related with both Li and electronall steps related with both Li and electron ransfers are still downhill in all free energy profiles as shown in Fig S1. The rate-determining step at the equilibrium potential is the same as that at U = 0 V. For the formation of lithium carbonate, the rate-determining step is *Li_2CO_2→*Li_2CO_3+ *CO, with its ΔG_{max}= +0.91 eV. While for the formation of lithium oxalate, the rate-determining step is *Li_2CO_2→*$Li_2C_2O_4$, with its ΔG_{max}= +0.15 eV.

In order to explore whether the results are sensitive to the concentration of the C defects, the catalytic activities of one to four C defects in Mo_2C were investigated by calculating the free energy changes of *Li_2CO_2 → *$Li_2C_2O_4$ and *Li_2CO_2 → *Li_2CO_3 + *CO, corresponding to −0.49 and −1.68 eV, −1.10 and −2.30 eV, −0.07 and −1.40 eV, respectively, as shown in Table S1. The higher free energy requirement for generating $Li_2C_2O_4$ suggests that increasing the C defects will reduce selectivity of Mo_2C for $Li_2C_2O_4$.

3.3. Electronic structure

3.3.1. Bader charge analysis

Bader charges can analyze the charge density around atoms, determine the number of valence electrons, and study the characteristics of charge transfer. The surface charge distribution of $Li_2C_2O_4$ and Li_2CO_3 on the V_C-Mo_2C surface was investigated using Bader charge analysis in this study. The Coulomb interaction between $Li_2C_2O_4$ and the V_C-Mo_2C

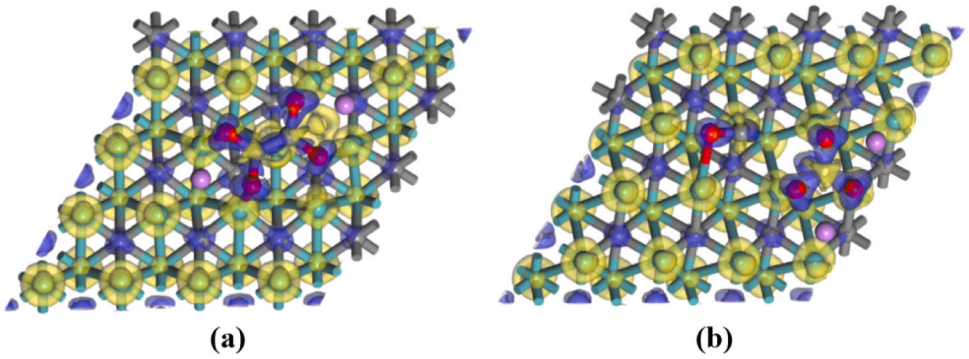

Fig. 4. The charge transfer situation of (a) $Li_2C_2O_4$ and (b) Li_2CO_3 on V_C-Mo_2C.

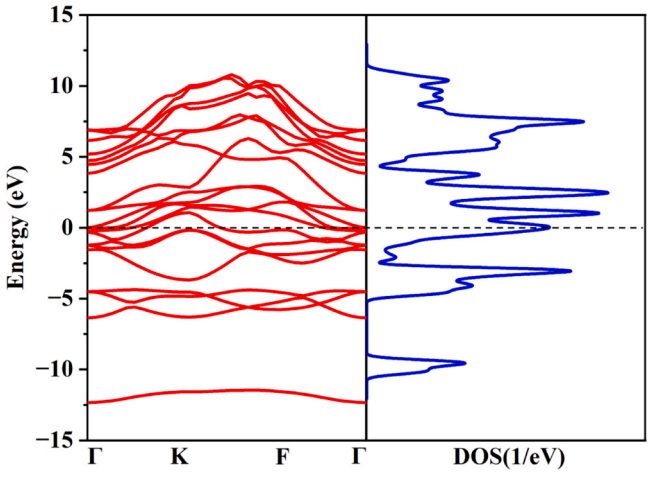

Fig. 5. Band structure and DOS for V_C-Mo_2C.

surface layer is a crucial determinant of the stability of $Li_2C_2O_4$ and the catalytic activity of V_C-Mo_2C [43,44]. The Bader charge analysis results for $Li_2C_2O_4$ and Li_2CO_3 on the V_C-Mo_2C configuration, are shown in the Fig. 4. Blue color indicates atoms with high electron affinity, while yellow color represents atoms prone to electron loss. As carbon is more electronegative than Mo, electrons tend to transfer from Mo atoms to C atoms. A significant charge interaction is observed between $Li_2C_2O_4$ and V_C-Mo_2C surfaces, indicating a strong interaction between them. Conversely, weak electron transfer occurs between Li_2CO_3 and V_C-Mo_2C, suggesting that nucleation of Li_2CO_3 on V_C-Mo_2C surface is challenging.

3.3.2. Band analysis

The band structure of V_C-Mo_2C was computed in this study, and its band structure and DOS in Fig. 5a. V_C-Mo_2C exhibits a complete absence of a band gap and possesses a zero bandgap width. This signifies that electrons can transfer from the valence band to the conduction band without encountering any energy barrier, thereby showcasing the exceptional electron transport capability of V_C-Mo_2C. With its elevated carrier concentration and conductivity at room temperature, V_C-Mo_2C emerges as a promising catalyst for Li-CO_2 batteries to facilitate CRR.

4. Conclusions

In this study, we employed density functional theory (DFT) to compute the Gibbs free energy changes of intermediate steps involved in the cathode reaction of Li-CO_2 batteries. Our research findings demonstrate that the free energy barrier for V_C-Mo_2C catalyst in generating Li_2CO_3 is higher compared to that for $Li_2C_2O_4$, indicating a greater selectivity in producing $Li_2C_2O_4$ as a product. The presence of C defects results in an increased exposure of Mo active sites, thereby enhancing the adsorption capability of V_C-Mo_2C on $Li_2C_2O_4$ and reducing the free energy associated with the generation of $Li_2C_2O_4$ through its reaction pathway. Furthermore, V_C-Mo_2C exhibits excellent conductivity and thermodynamic stability, ensuring both sustainability and efficiency throughout the catalytic process. Consequently, V_C-Mo_2C holds significant potential as an efficient cathode catalyst for Li-CO_2 batteries.

CRediT authorship contribution statement

Yan Lixiang: Writing – original draft. **Zhao Tingting:** Writing – original draft, Funding acquisition. **Yan Likai:** Writing – review & editing. **Su Yukang:** Investigation. **Li Ao:** Investigation. **Xiong Yiyu:** Conceptualization. **Nie Yanmei:** Funding acquisition. **Song Liubin:** Writing – review & editing, Funding acquisition. **Qiu Xueying:** Funding acquisition.

Declaration of Competing Interest

The authors declare that they have no known competing financial interests or personal relationships that could have appeared to influence the work reported in this paper.

Acknowledgements

This work was financially supported by National Natural Science Foundation of China (21501015, 52204319, 22405026), Natural Science Foundation of Hunan Province of China (2022JJ30604, 2023JJ40012), Hunan Provincial Key Laboratory of Regional Hereditary Birth Defects Prevention and Control (Grant No. HPKL2023034).

Appendix A. Supporting information

Supplementary data associated with this article can be found in the online version at doi:10.1016/j.fub.2025.100058.

Data availability

No data was used for the research described in the article.

References

[1] T.T. Zhao, L.X. Yan, F.L. Tang, M.Z. Xiao, Y. Tan, L.B. Song, Z.L. Xiao, L.J. Li, Research progress on design strategies and reaction mechanisms of catalysts for photo−assisted Li−CO_2 batteries, CIESC J. 75 (2024) 1750–1764, https://doi.org/10.11949/0438-1157.20240091.
[2] L. Chen, J. Zhou, J. Zhang, G. Qi, B. Wang, J. Cheng, Copper indium sulfide enables Li-CO_2 batteries with boosted reaction kinetics and cycling stability, Energy Environ. Mater. 6 (2023) e12415, https://doi.org/10.1002/eem2.12415.
[3] L. Huang, H. Zhao, Y. Zhao, Z. Chen, S. Sun, Z. Zhang, S. Liao, Atomically dispersed Cu and Cr on N-doped hollow carbon nanocages for synergistic promotion of high-performance Li–CO_2 batteries, Chem. Eng. J. 493 (2024) 152723, https://doi.org/10.1016/j.cej.2024.152723.

[4] Z. Zhang, X. Xiao, A. Yan, Z. Zhang, P. Tan, Unravelling the capacity degradation mechanism of thick electrodes in lithium-carbon dioxide batteries via visualization and quantitative techniques, Adv. Funct. Mater. (2024) 2407422, https://doi.org/10.1002/adfm.202407422.

[5] J. Zhou, T. Wang, L. Chen, L. Liao, Y. Wang, S. Xi, B. Chen, T. Lin, Q. Zhang, C. Ye, X. Zhou, Z. Guan, L. Zhai, Z. He, G. Wang, J. Wang, J. Yu, Y. Ma, P. Lu, Y. Xiong, S. Lu, Y. Chen, B. Wang, C.-S. Lee, J. Cheng, L. Gu, T. Zhao, Z. Fan, Boosting the reaction kinetics in aprotic lithium-carbon dioxide batteries with unconventional phase metal nanomaterials, Proc. Natl. Acad. Sci. 119 (2022) e2204666119, https://doi.org/10.1073/pnas.2204666119.

[6] L. Zhou, H. Wang, K. Zhang, Y. Qi, C. Shen, T. Jin, K. Xie, Fast decomposition of Li_2CO_3/C actuated by single-atom catalysts for Li-CO_2 batteries, Sci. China Mater. 64 (2021) 2139–2147, https://doi.org/10.1007/s40843-020-1638-6.

[7] Q.Q. Hao, Z. Zhang, Y. Mao, K.X. Wang, Catalysts for Li−CO_2 batteries: from heterogeneous to homogeneous, ChemNanoMat 8 (2022) e202100381, https://doi.org/10.1002/cnma.202100381.

[8] Y. Jin, Y. Liu, L. Song, J. Yu, K. Li, M. Zhang, J. Wang, Interfacial engineering in hollow NiS_2/FeS_2-NSGA heterostructures with efficient catalytic activity for advanced Li-CO_2 battery, Chem. Eng. J. 430 (2022) 133029, https://doi.org/10.1016/j.cej.2021.133029.

[9] J. Wang, S. Tian, Y. Lin, H. Song, N. Feng, G. Yang, Q. Zhao, Recent advancement in designing catalysts for rechargeable Li–CO_2 batteries, Catal. Sci. Technol. 14 (2024) 2991–3000, https://doi.org/10.1039/D4CY00325J.

[10] A.K. Chourasia, K.M. Naik, C.S. Sharma, Exploring the synergistic effects of chemical activation and N-doping in carbon nanospheres for advanced Li–CO_2 Mars batteries, Carbon 218 (2024) 118754, https://doi.org/10.1016/j.carbon.2023.118754.

[11] K.M. Naik, A.K. Chourasia, M. Shavez, C.S. Sharma, Bimetallic RuNi electrocatalyst coated MWCNTs cathode for an efficient and stable Li−CO_2 and Li−CO_2 mars batteries performance with low overpotential 16 (2023) e202300734, https://doi.org/10.1002/cssc.202300734.

[12] S. Wang, H. Song, T. Zhu, J. Chen, Z. Yu, P. Wang, L. Yu, J. Xu, H. Zhou, K. Chen, An ultralow-charge-overpotential and long-cycle-life solid-state Li-CO_2 battery enabled by plasmon-enhanced solar photothermal catalysis, Nano Energy 100 (2022) 107521, https://doi.org/10.1016/j.nanoen.2022.107521.

[13] T. Zhu, S. Wang, Z. Yu, H. Song, J. Xu, K. Chen, High-performance Li-CO_2 battery based on carbon-free porous Ru@QNFs cathode, Small 19 (2023) 2301498, https://doi.org/10.1002/smll.202301498.

[14] D. Cao, C. Tan, Y. Chen, Oxidative decomposition mechanisms of lithium carbonate on carbon substrates in lithium battery chemistries, Nat. Commun. 13 (2022) 4908, https://doi.org/10.1038/s41467-022-32557-w.

[15] Y. Liu, P. Shu, M. Zhang, B. Chen, Y. Song, B. Lu, R. Mao, Q. Peng, G. Zhou, H. M. Cheng, Uncovering the geometry activity of spinel oxides in Li-CO_2 battery reactions, ACS Energy Lett. 9 (2024) 2173–2181, https://doi.org/10.1021/acsenergylett.4c00603.

[16] K.M. Naik, A. Kumar Chourasia, C.S. Sharma, Nano-interface engineering of $NiFe_2O_4$/MoS_2/MWCNTs heterostructure catalyst as cathodes in the Long-Life reversible Li-CO_2 Mars batteries, Chem. Eng. J. 490 (2024) 151729, https://doi.org/10.1016/j.cej.2024.151729.

[17] K.M. Naik, A.K. Chourasia, C.S. Sharma, N, S Co-doped carbon anchored Co_9S_8 cathode: advancing sustainable energy through efficient Li–CO_2 Mars batteries, J. Power Sources 608 (2024) 234623, https://doi.org/10.1016/j.jpowsour.2024.234623.

[18] Y. Xu, H. Gong, H. Ren, X. Fan, P. Li, T. Zhang, K. Chang, T. Wang, J. He, Highly efficient Cu-porphyrin-based metal–organic framework nanosheet as cathode for high-rate Li-CO_2 battery, Small 18 (2022) 2203917, https://doi.org/10.1002/smll.202203917.

[19] Y. Chen, J. Li, B. Lu, Y. Liu, R. Mao, Y. Song, H. Li, X. Yu, Y. Gao, Q. Peng, X. Qi, G. Zhou, Activated Co in thiospinel boosting Li_2CO_3 decomposition in Li−CO_2 batteries, Adv. Mater. 36 (2024) 2406856, https://doi.org/10.1002/adma.202406856.

[20] Y. Liu, Z. Zhang, J. Tan, B. Chen, B. Lu, R. Mao, B. Liu, D. Wang, G. Zhou, H. M. Cheng, Deciphering the contributing motifs of reconstructed cobalt (II) sulfides catalysts in Li-CO_2 batteries, Nat. Commun. 15 (2024) 2167, https://doi.org/10.1038/s41467-024-46465-8.

[21] R. Mao, Y. Liu, P. Shu, B. Lu, B. Chen, Y. Chen, Y. Song, Y. Jia, Z. Zheng, Q. Peng, G. Zhou, Tailoring Li_2CO_3 configuration and orbital structure of CoS to improve catalytic activity and stability for Li-CO_2 batteries, EcoMat 6 (2024) e12449, https://doi.org/10.1002/eom2.12449.

[22] X. Ji, Y. Liu, Z. Zhang, J. Cui, Y. Fan, Y. Qiao, Carbon nanotubes with CoNi alloy nanoparticles growing on porous carbon substrate as cathode for Li-CO_2 batteries, J. Colloid Interface Sci. 655 (2024) 693–698, https://doi.org/10.1016/j.jcis.2023.11.038.

[23] Y. Hou, J. Wang, L. Liu, Y. Liu, S. Chou, D. Shi, H. Liu, Y. Wu, W. Zhang, J. Chen, Mo_2C/CNT: an efficient catalyst for rechargeable Li–CO_2 batteries, Adv. Funct. Mater. 27 (2017) 1700564, https://doi.org/10.1002/adfm.201700564.

[24] J. Zhou, X. Li, C. Yang, Y. Li, K. Guo, J. Cheng, D. Yuan, C. Song, J. Lu, B. Wang, A quasi-solid-state flexible fiber-shaped Li–CO_2 battery with low overpotential and high energy efficiency, Adv. Mater. 31 (2019) 1804439, https://doi.org/10.1002/adma.201804439.

[25] Y. Hou, J. Wang, L. Liu, Y. Liu, S. Chou, D. Shi, H. Liu, Y. Wu, W. Zhang, J. Chen, Mo_2C/CNT: an efficient catalyst for rechargeable Li–CO_2 batteries 27 (2017) 1700564, https://doi.org/10.1002/adfm.201700564.

[26] C. Yang, K. Guo, D. Yuan, J. Cheng, B. Wang, Unraveling reaction mechanisms of Mo_2C as cathode catalyst in a Li-CO_2 battery, J. Am. Chem. Soc. 142 (2020) 6983–6990, https://doi.org/10.1021/jacs.9b12868.

[27] Z. Chen, M. Yuan, Z. Tang, H. Zhu, G. Zeng, Magnetron sputtering of platinum on nitrogen-doped polypyrrole carbon nanotubes as an efficient and stable cathode for lithium–carbon dioxide batteries, Phys. Chem. Chem. Phys. 25 (2023) 7662–7668, https://doi.org/10.1039/D3CP00116D.

[28] J. Wang, N. Feng, S. Zhang, Y. Lin, Y. Zhang, J. Du, S. Tian, Q. Zhao, G. Yang, Improving the rechargeable Li-CO_2 battery performances by tailoring oxygen defects on Li-Ni-Co-Mn multi-metal oxide catalysts recycled from spent ternary lithium-ion batteries, Adv. Sci. 11 (2024) 2402892, https://doi.org/10.1002/advs.202402892.

[29] J. Hu, C. Su, R. Li, B. Li, Z. Hou, Y. Fan, Y. Pan, J. Liu, A. Hu, High-performance Li-CO_2 batteries enabled by synergistic interaction of iron dopant-modulated catalysts and nitrogen-modified substrates, J. Alloy. Compd. 976 (2024), https://doi.org/10.1016/j.jallcom.2023.173146.

[30] X. Tian, M. Xu, Y. Li, H. Liu, B. Cao, R.A. Soomro, P. Zhang, B. Xu, Mild oxidation regulating the surface of Mo_2CTx MXene to enhance catalytic activity for low overpotential and long cycle life Li-CO_2 batteries, Chem. Eng. J. 489 (2024) 151510, https://doi.org/10.1016/j.cej.2024.151510.

[31] J. Han, H. Wu, R. Song, W. Mao, D. Wang, D. Liu, Defect-rich porous carbon as a metal-free catalyst for high-performance Li-CO_2 batteries, Electrochim. Acta 477 (2024) 143779, https://doi.org/10.1016/j.electacta.2024.143779.

[32] B. Delley, An all-electron numerical method for solving the local density functional for polyatomic molecules, J. Chem. Phys. 92 (1990) 508–517, https://doi.org/10.1063/1.458452.

[33] X. Nie, W. Luo, M.J. Janik, A. Asthagiri, Reaction mechanisms of CO_2 electrochemical reduction on Cu(111) determined with density functional theory, J. Catal. 312 (2014) 108–122, https://doi.org/10.1016/j.jcat.2014.01.013.

[34] J.P. Perdew, Y. Wang, Accurate and simple analytic representation of the electron-gas correlation energy, Phys. Rev. B 97 195128 (2018), https://doi.org/10.1103/PhysRevB.98.079904.

[35] B. Delley, Hardness conserving semilocal pseudopotentials, Phys. Rev. B 66 (2002) 155125, https://doi.org/10.1103/PhysRevB.66.155125.

[36] S. Grimme, Semiempirical GGA-type density functional constructed with a long-range dispersion correction, J. Comput. Chem. 27 (2006) 1787–1799, https://doi.org/10.1002/jcc.20495.

[37] A. Klamt, G. Schüürmann, COSMO: a new approach to dielectric screening in solvents with explicit expressions for the screening energy and its gradient, J. Chem. Soc. Perkin Trans. 2 (1993) 799–805, https://doi.org/10.1039/P29930000799.

[38] J.K. Nørskov, J. Rossmeisl, A. Logadottir, L. Lindqvist, J.R. Kitchin, T. Bligaard, H. Jónsson, Origin of the overpotential for oxygen reduction at a fuel-cell cathode, J. Phys. Chem. B 108 (2004) 17886–17892, https://doi.org/10.1021/jp047349j.

[39] A.A. Peterson, F. Abild-Pedersen, F. Studt, J. Rossmeisl, J.K. Nørskov, How copper catalyzes the electroreduction of carbon dioxide into hydrocarbon fuels, Energy Environ. Sci. 3 (2010) 1311–1315, https://doi.org/10.1039/C0EE00071J.

[40] H. Wu, Z. Guo, J. Zhou, Z. Sun, Vacancy-mediated lithium adsorption and diffusion on MXene, Appl. Surf. Sci. 488 (2019) 578–585, https://doi.org/10.1016/j.apsusc.2019.05.311.

[41] C. Shao, W. Wang, Y. Cheng, Synergetic effect of vacancy and dual-metals on defective V_2CO_2 MXene as efficient catalysts for nitrogen reduction reaction, Appl. Surf. Sci. 665 (2024) 160295, https://doi.org/10.1016/j.apsusc.2024.160295.

[42] X. Liu, R. Lu, Q. Liu, M. Zhou, X. Liao, Z. Wang, Y. Zhao, Reaction mechanisms and activities of dual-metal sites for Li-O_2 batteries: the first-principle investigation, Appl. Surf. Sci. 616 (2023) 156493, https://doi.org/10.1016/j.apsusc.2023.156493.

[43] H.J. Kim, S.C. Jung, Y.K. Han, S.H. Oh, An atomic-level strategy for the design of a low overpotential catalyst for Li−O_2 batteries, Nano Energy 13 (2015) 679–686, https://doi.org/10.1016/j.nanoen.2015.03.030.

[44] M. Lee, Y. Hwang, K.H. Yun, Y.C. Chung, Greatly improved electrochemical performance of lithium–oxygen batteries with a bimetallic platinum–copper alloy catalyst, J. Power Sources 288 (2015) 296–301, https://doi.org/10.1016/j.jpowsour.2015.04.143.